



New measurements of kaonic helium-4 L-series X-rays yields in gas with the SIDDHARTINO setup

D.L. Sirghi^{a,b,c,*}, H. Shi^d, C. Guaraldo^a, F. Sgaramella^{a,**}, C. Amsler^d,
M. Bazzi^a, D. Bosnar^e, A.M. Bragadireanu^c, M. Carminati^{f,g},
M. Cargnelli^d, A. Clozza^a, G. Deda^{f,g}, L. De Paolis^a, R. Del Grande^{a,h},
L. Fabbietti^h, C. Fiorini^{f,g}, M. Iliescu^a, M. Iwasakiⁱ, J. Marton^d,
M. Miliucci^a, P. Moskal^j, F. Napolitano^a, S. Niedzwiecki^j, H. Ohnishi^k,
K. Piscicchia^{b,a}, Y. Sada^k, A. Scordo^a, M. Silarski^j, F. Sirghi^{a,c},
M. Skurzok^j, A. Spallone^a, K. Toho^k, M. Tüchler^{d,l}, O. Vazquez Doce^a,
J. Zmeskal^d, C. Yoshida^k, C. Curceanu^a

^a INFN, Laboratori Nazionali di Frascati, Via E. Fermi 54, I-00044 Frascati (Roma), Italy

^b Centro Ricerche Enrico Fermi - Museo Storico della Fisica e Centro Studi e Ricerche "Enrico Fermi", Via Panisperna 89A, 00184, Rome, Italy

^c IFIN-HH, Institutul National pentru Fizica si Inginerie Nucleara Horia Hulubbei, Reactorului 30, Magurele, Romania
^d Stefan-Meyer-Institut für Subatomare Physik, Boltzmannngasse 3, 1090 Wien, Austria

^e Department of Physics, Faculty of Science, University of Zagreb, Bijenicka 32, HR-10000 Zagreb, Croatia

^f Politecnico di Milano, Dipartimento di Elettronica, Informazione e Bioingegneria, Piazza L. da Vinci 32, 20133 Milano, Italy

^g INFN Sezione di Milano, Via Celoria 16, 20133 Milano, Italy

^h Physik Department E62, Technische Universität München, James-Frank Straße 1, D-85748 Garching, Germany

ⁱ RIKEN, Institute of Physical and Chemical Research, 2-1 Hirosawa, Wako, Saitama 251-0198, Japan

^j Institute of Physics, Jagiellonian University, prof. Stanisława Lojasiewicza 11, 30-438, Krakow, Poland

^k Research Center for Electron Photon Science (ELPH), Tohoku University, Sendai 982-0826, Japan

^l University of Vienna, Vienna Doctoral School in Physics, Boltzmannngasse 5, 1090 Vienna, Austria

Received 11 August 2022; received in revised form 14 October 2022; accepted 27 October 2022

Available online 31 October 2022

* Corresponding author at: INFN, Laboratori Nazionali di Frascati, Via E. Fermi 54, I-00044 Frascati (Roma), Italy.

** Corresponding author.

E-mail addresses: Diana.Laura.Sirghi@Inf.infn.it (D.L. Sirghi), francesco.sgaramella@Inf.infn.it (F. Sgaramella).

Abstract

The L -series X-rays transitions of the kaonic helium-4 exotic atom were measured by SIDDHARTINO, the reduced configuration of the SIDDHARTA-2 experiment, at the DAΦNE collider of INFN-LNF, with gaseous ^4He targets at densities of 1.90 g/l and 0.82 g/l, corresponding to 1.5% and 0.66%, respectively, of the liquid helium-4 density. The absolute yields for the L_α transition are determined to be 0.15 ± 0.03 and 0.12 ± 0.03 , for the two target densities. The yields for the L_β and L_γ transitions are presented relatively to that of the L_α transition. These results are compatible with the yields measured by the SIDDHARTA experiment at the densities of 1.65 g/l and 2.15 g/l and contribute to refine the cascade models describing the de-excitation of kaonic atoms as function of density.

© 2022 Elsevier B.V. All rights reserved.

Keywords: Kaonic atom; Kaonic helium-4; Atomic cascade; X-ray spectroscopy

1. Introduction

The X-ray spectroscopy of kaonic atoms is a well established method to study the strong interaction between negatively charged kaon (K^-) and nuclei at low-energy. From the level energy shifts and broadenings with respect to the values determined from the electromagnetic interaction only, it is possible to extract information on the strong interaction between the kaon and the nucleus at threshold. Such information is being used for a better understanding of the Quantum Chromodynamics effective theories in the non-perturbative regime in systems with strangeness [1–7].

Beyond the study of the strong interaction, kaonic atoms have been investigated also to understand the mechanisms of de-excitation, after the kaon is captured in a highly-excited level and before it reaches the lower-lying levels by cascading and is absorbed by the nucleus. Moreover, the yields of the transitions of kaonic X-rays, defined as the number of X-rays generated per stopped kaon, are a key factor to estimate the final detection efficiency of the setup. The early cascade models of Leon and Bethe [8] and Borie and Leon [9] introduced the Stark mixing effect, that causes a negatively charged particle to be absorbed by the nucleus from highly-excited atomic states, so reducing the yields of the transitions to the lower-lying states. The effect was included as free parameters, to be tuned from different exotic atoms as a function of density, and became an essential ingredient of any cascade model.

However, while for hydrogen the Stark mixing plays a major role and the model of Jensen [10] reproduces correctly the experimental yield measured by KEK [11] for the $2p \rightarrow 1s$ kaonic hydrogen transition, the case of helium-4 is completely different, since the Stark effect shows a drastic difference. In a helium atom, when a kaon is captured in a highly excited state, it immediately de-excites by the internal Auger process, emitting the second electron and forming a hydrogen-like positive ion $(K^- \text{He})^+$. Indeed, the kaonic hydrogen is neutral and small, which makes it easy to penetrate the surrounding atoms and then experience their strong electric field. This is not the case for kaonic ions. The newly formed $(K^- \text{He})^+$ ion induces a molecular electric field by polarizing the neighbor atoms, an effect called “molecular Stark mixing”. Moreover, the $(K^- \text{He})^+$ ion, in three-body collisions with other neighbor neutral atoms, forms, on its turn, a molecular positive ion state, a process called “Molecular Ion Formation (MIF)”. The MIF then de-excites by external Auger process, a process competing with radiative transitions. In addition to MIF, the initial kaonic-helium ion, within the environment of neighbor neutral atoms, gives rise

to the so-called ‘‘Coulomb de-excitation’’, a collisional process that transforms potential energy in kinetic energy [12,13]. As far as the cascade models are concerned, Koike and Akaishi [14] developed, nearly 25 years ago, a model for kaonic helium including both the molecular Stark mixing and the MIF process. By tuning the rate of the first effect and the strength of the second, they reproduced the only experimental point - at liquid helium-4 density - measured at that time by Baird et al., [15] in 1983, and, as well, they reproduced the antiprotonic-helium-4 data in liquid helium. The calculations of Koike and Akaishi have been performed sixteen years before the publication of the SIDDHARTA experiment on ‘‘L-series transitions in Kaonic Helium with a gaseous target’’ [16] at the densities of 2.15 g/l (1.7% LHeD) and 1.65 g/l (1.32% LHeD). Unfortunately, the calculations did not reproduce the experimental data measured by SIDDHARTA. In particular, the 2.15 g/l density point, to which corresponds a measured yield of $17.2^{+2.6}_{-9.5}\%$ for the $3d \rightarrow 2p$ transition, is not well reproduced by the density dependence yield from the Koike and Akaishi’s calculations, which instead obtains the value of 23%. Consequently, actually it is not possible to define the density dependence of the yields of the transitions in kaonic helium over the whole density scale, from liquid to gas. With the specific aim to provide more inputs to cascade calculations, two other measurements in gaseous targets, at 1.90 g/l (1.52% LHeD) and 0.82 g/l (0.66% LHeD) were performed with the SIDDHARTINO setup [17] - employing one sixth of the X-ray detectors of the SIDDHARTA-2 experiment, at the DAΦNE collider of INFN-LNF, so to make available, overall, four experimental points at low density.

In this paper the SIDDHARTINO experimental results on the yields of the kaonic helium-4 L-series X-rays are presented, measured at the gas target densities of 1.90 g/l and 0.82 g/l. In section 2, the experimental setup is described, with focus on the kaon paths, from their generation at the beams collision point to the stopping inside the target. In section 3, the kaonic helium-4 L-series yields are derived for the two densities by using Monte Carlo simulations. Finally, in section 4, the results and their importance are discussed.

2. The SIDDHARTINO experiment

The SIDDHARTINO experiment, installed in the interaction point (IP) of the DAΦNE collider, was the pilot setup for the SIDDHARTA-2 experiment, which aims to measure the kaonic deuterium transitions to the ground state. The run was performed, with the goal to assess and optimize the performances of the machine and the experimental apparatus via a measurement of the kaonic helium transitions to the 2p level, made possible by the much higher yields of these transitions [16] compared to the expected kaonic deuterium ones [5].

In the DAΦNE collider, due to the crossing angle of 50 mrad between the electron and positron beams, the ϕ -meson has a transverse momentum of 25.48 MeV/c along the horizontal plane of the colliding beams (ϕ -boost towards the center of the collider rings). Therefore, the back-to-back kaons momenta, resulting from $\phi \rightarrow K^+ K^-$ decays, with 49.2% branching ratio, have a small angular dependence. The emitted kaons have a kinetic energy of about ~ 16 MeV, making them suitable to be stopped in a low density targets.

A schematic view of the SIDDHARTINO apparatus is shown in Fig. 1. The beam pipe surrounding the IP region, customized for the experiment, has an inner diameter of 58.3 mm and it is made of 150 μm thick pure aluminium with a 500 μm carbon fiber reinforcement, uniform along the circumference. The special beam pipe materials are chosen to reduce background radiation originated from particles lost from the beams due to Touschek effect.

A pair of 1.5 mm thick plastic scintillators, placed about 12 cm above and below the IP, read by photo-multipliers, act as kaons detector. The kaon trigger, defined by the coincidence

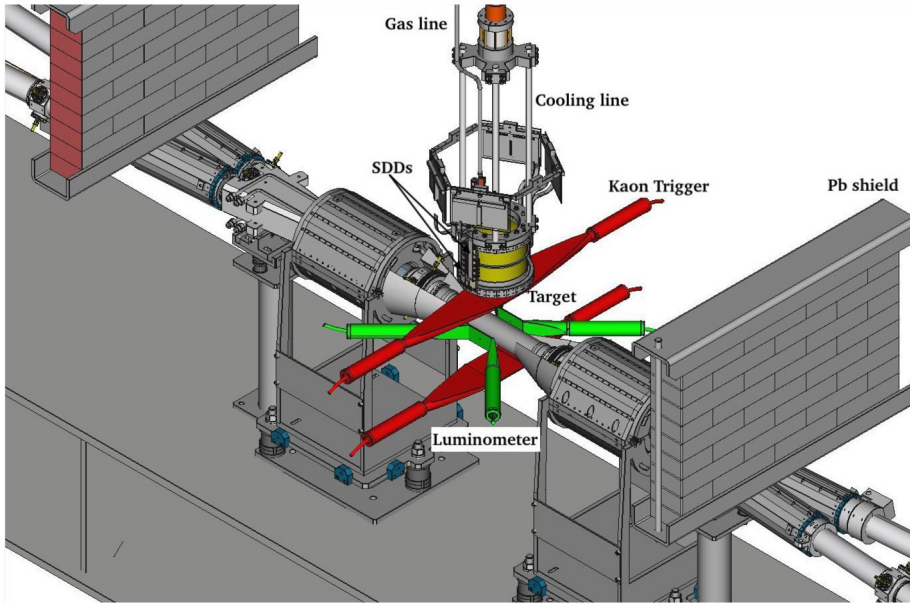


Fig. 1. A schematic view of the SIDDHARTINO apparatus.

between the two scintillators, gives an identification of the back-to-back K^+K^- pair directed towards the target. A clear separation between the kaons and the Minimum Ionizing Particles (MIPs), namely particles whose energy loss through matter is close to its minimum, is achieved using the time-of-flight information [18–20]. A vacuum chamber, placed above the IP, contains a cylindrical target cell made of Kapton polyimide ($C_{22}H_{10}N_2O_5$), 125 mm in height and 144 mm in diameter. The target is cooled to about 23 K at a pressure of about 1.2 bar, to obtain (1.52% LHeD), corresponding to 1.90 g/l, and a pressure of about 0.42 bar to obtain (0.66% LHeD), corresponding to 0.82 g/l. The X-rays emitted from the radiative transitions of kaonic atoms in the gas target, are detected through the dedicated Silicon Drift Detector (SSD) system developed by the SIDDHARTA-2 collaboration [21,22]. Within SIDDHARTINO, the target is surrounded by 8 SDDs arrays, out of a total of 48 arrays, for a total number of 64 SDDs, each one with an effective area of 0.64 cm^2 . Multiple foils of copper and titanium are placed inside the setup for the energy calibration of the SDDs. These foils are irradiated with an X-ray tube from the lateral side of the setup every few hours in between the measurements with beam. A detailed description of the configuration of the target and the SDDs, the calibration procedure and performance of the SDDs for the SIDDHARTINO measurement can be found in [23,17,24,25]. After passing through all materials of the setup, the kaons need to be additionally slowed down. In order to decrease the K^- momentum such as to center the Bragg peak inside the gas target, a degrader made of Mylar is placed below the upper scintillator of the kaon detector. To compensate the small angular dependence of the low-momenta K^+K^- pairs due to the ϕ -boost, a stepwise degrader, made of Mylar, thicker towards the center of the accelerator rings, is used. The optimization of the shape and thickness of the degrader was first determined from the MC simulations and then finally tuned by experimental data [17].

During the beam time dedicated with the SIDDHARTINO apparatus to the commissioning of the detectors and setup, the kaonic helium-4 X-rays were measured and the degrader thickness

optimized. A new result on the shift and width of the $2p$ atomic level of kaonic helium-4 atom was obtained [17]. The absolute yield for the L_α transition, and the relative yields for the L_β and for the L_γ ones with respect to the L_α at 1.90 g/l and 0.82 g/l target densities, respectively, were determined. The procedure to evaluate the yields and their experimental values are given in Section 3.

3. The yields of $K^-4\text{He}$ L-series X-rays

To measure the absolute yield Y of the L_α X-ray transition for kaonic helium-4, the detection efficiency of kaonic X-rays, ϵ^{EXP} , obtained by normalizing the number of detected X-ray events $N_{X\text{-ray}}$ to the number of kaon triggers N_{ktrg} and to the surface areas of the SDDs used in the analysis, was firstly determined. From the SIDDHARTINO Monte Carlo simulations, the Monte Carlo efficiency, ϵ^{MC} , given by the ratio of the number of detected X-ray events $N_{X\text{-ray}}^{MC}$ to the number of kaon triggers in the simulation N_{ktrg}^{MC} , assuming that each stopped kaon leads to a subsequent kaonic X-ray event, was evaluated.

The absolute yield Y of the L_α X-ray transition for the kaonic helium-4 is then given by:

$$Y = \frac{\epsilon^{EXP}}{\epsilon^{MC}} = \frac{N_{X\text{-ray}}/N_{ktrg}}{N_{X\text{-ray}}^{MC}/N_{ktrg}^{MC}}. \quad (1)$$

The same notations have been used by SIDDHARTINO to extract the yields of X-rays from kaonic atoms arising from the interaction of kaons with Kapton foils [20], kaonic helium-3, at the density of 0.96 g/l, kaonic helium-4 at the densities of 1.65 g/l and 2.15 g/l [16], and kaonic hydrogen at the density of 1.3 g/l [26].

3.1. Data analysis

To obtain the number of kaon triggers N_{ktrg} , identified by the coincidence of a pair of kaons at the top and bottom scintillators of the kaons detector, the timing information to separate kaons from MIPs was used. The time-of-flight difference and the timing resolution allow to define the kaons with less than 1% contamination from the MIPs. More details on the data analysis are discussed in a separate paper [17]. The energy calibration for each individual SDD was performed using the fluorescence lines of Ti and Cu, at the energies of 4.5 keV and of 8.1 keV, respectively, following the same procedure introduced in [23,25]. From the data corresponding to 33 SDDs out of the 64 SDDs installed in the setup, which were operating stably with good energy resolution ($157.0 \text{ (stat)} \pm 0.4 \text{ (syst)} \text{ eV}$ (FWHM) at 6.4 keV), the X-ray events correlated to the kaon trigger timing were selected and the X-ray energy spectra for optimal degrader runs were obtained. Fig. 2, shows the spectra of: (a) the 0.82 g/l target density measurement obtained with 4.3 pb^{-1} integrated luminosity, in an acquisition time of 70 hours; (b) the 1.90 g/l target density measurement obtained with 9.5 pb^{-1} integrated luminosity, in an acquisition time of 125 hours. To fit each energy spectrum, the L_α , L_β , and L_γ lines of kaonic helium-4, each represented by a Gaussian function, were included. The strong interaction width of the $2p$ level was set to zero in this analysis, since the strong interaction broadening is negligible [17]. A common parameter for the energy shift for the $2p$ state was introduced for all the three transitions. The intensities of the L_β and L_γ transitions are given as ratios to the L_α transition. The background includes other kaonic X-rays coming from the K^- stopped inside the Kapton walls of the target cell, represented by Gaussian functions, with their transition energies set to the values used in

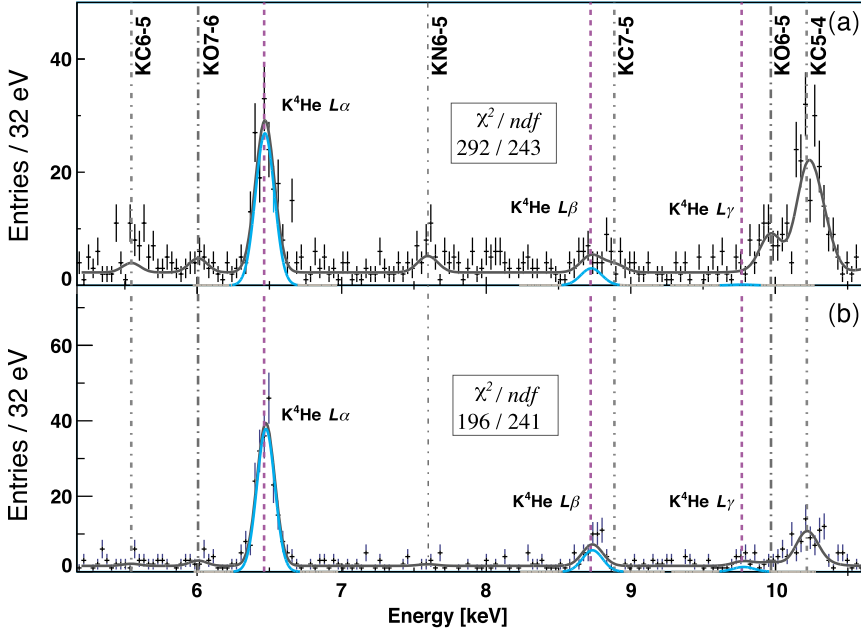


Fig. 2. X-ray kaonic helium-4 spectra measured by SIDDHARTINO for: (a) 0.82 g/l target gas density; (b) 1.90 g/l target gas density. The kaonic helium-4 peaks L_α , L_β and L_γ are shown. Several kaonic atom X-ray lines produced in the Kapton foils are also shown: Kaonic Carbon 6 \rightarrow 5, Kaonic Oxygen 7 \rightarrow 6, Kaonic Nitrogen 6 \rightarrow 5, Kaonic Carbon 7 \rightarrow 5, Kaonic Oxygen 6 \rightarrow 5, Kaonic Carbon 5 \rightarrow 4 transitions. The solid line shows the fit function of the spectrum. The blue line shows the L series L_α , L_β and L_γ kaonic helium-4 components. (For interpretation of the color(s) in the figure(s), the reader is referred to the web version of this article.)

Table 1

The number of L_α X-ray events and the relative intensities of the L_β , L_γ transitions, with their statistical error, obtained from the SIDDHARTINO measurement.

	1.90 g/l	0.82 g/l
L_α X-ray events	191 ± 14	146 ± 12
L_β/L_α	0.162 ± 0.031	0.114 ± 0.032
L_γ/L_α	0.031 ± 0.012	not detected

[20], indicated with the dotted lines in the figure. A second-order polynomial function is used to represent the background over the fitted energy range (5 \div 10.5 keV). The resulting fit functions and the components corresponding to the kaonic helium-4 X-rays, are plotted in the energy spectra.

The number of L_α X-ray events obtained from the fit and the relative intensities of the L_β and L_γ with respect to L_α are listed in Table 1, with their statistical error. For the 1.90 g/l target density, the detection efficiency ϵ^{EXP} of L_α is (16.26 ± 1.26) events per million kaon triggers per cm^2 SDD. For the 0.82 g/l target density, the detection efficiency ϵ^{EXP} of L_α is (5.8 ± 0.6) events per million kaon triggers per cm^2 SDD.

Table 2

The absolute yield of the kaonic helium-4 L_α transition and the relative yields of the L_β and L_γ corrected by detectors efficiencies, obtained with the SIDDHARTINO setup.

Density	1.90 g/l	0.82 g/l
L_α yield	0.148 ± 0.027	0.126 ± 0.023
L_β/L_α	0.193 ± 0.042	0.133 ± 0.037
L_γ/L_α	0.035 ± 0.015	not detected

3.2. Monte Carlo simulation for ϵ^{MC}

Dedicated Monte Carlo (MC) simulations, using GEANT4 toolkit, were performed to evaluate the fraction of kaons stopping in the gas targets, needed to extract the absolute X-ray yields. The X-ray detection efficiencies of the SDDs, ϵ^{MC} , were extracted from the simulations. Kaonic atom X-rays were generated at the position where the K^- stopped, and were isotropically emitted with a 100% yield for each transition and each kaonic atom. In this way one can directly compare the ratios between $N_{\text{X-ray}}$ and N_{trg} from the experiment and from the simulation. In the simulation all the materials and geometries used in the experiment were reproduced. The simulation starts at the DAΦNE IP with a ϕ -meson, whose initial position and boost momentum are derived from the crossing angle, the dimensions of the interaction region, and the momentum bite of the e^+e^- beams. The subsequent K^+K^- pair carries the boost momentum of the ϕ , and its momentum direction follows the angular distribution, as a result of a spin-one particle decaying into two spin-zero particles. The number of kaon triggers $N_{\text{trg}}^{\text{MC}}$ was calculated by requiring the coincidence between the top and bottom kaon detectors. The number of kaonic helium-4 events detected by the SDDs, $N_{\text{X-ray}}^{\text{MC}}$, was normalized to the number of kaon triggers $N_{\text{trg}}^{\text{MC}}$ and to the total surface area of the SDDs in MC. The efficiency (ϵ^{MC}) in the simulation is defined as the number of X-rays detected by the SDDs divided by the number of kaon triggers. The detection efficiencies ϵ^{MC} for the two target densities turned to be (110 ± 18) events per million kaon triggers per cm^2 SDD for the 1.90 g/l target density and (46 ± 7) events per million kaons trigger per cm^2 SDD for the 0.82 g/l target density. The errors come from systematic uncertainties related to the setup material composition, beam features, beam pipe dimensions and densities.

4. Results and discussions

By applying the values obtained from sections 3.1 and 3.2 into Eq. (1), the absolute yield for L_α of kaonic helium-4 X-ray was determined to be:

$$Y_{L_\alpha} = \frac{16.26 \pm 1.26}{110 \pm 18} = 0.148 \pm 0.027 \quad (2)$$

at 1.90 g/l target density, and

$$Y_{L_\alpha} = \frac{5.8 \pm 0.6}{46 \pm 7} = 0.126 \pm 0.023 \quad (3)$$

at 0.82 g/l target density, where the statistic and systematic errors were added quadratically.

In Table 2, the absolute yields of the kaonic helium-4 L_α transition and the relative yields of the L_β and L_γ , corrected by detector efficiencies, obtained with the SIDDHARTINO setup are given.

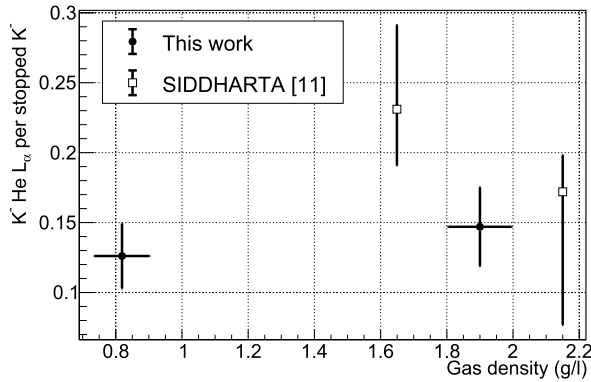


Fig. 3. The L_{α} X-ray yield of $K^{-4}\text{He}$ as function of the target density from all gaseous target measurements: this work (filled dots) and SIDDHARTA [16] (hollow squares).

In Fig. 3, the absolute yields for the kaonic helium-4 L_{α} X-rays measured by SIDDHARTINO are plotted together with the previous SIDDHARTA results [16] in gas. The helium gas density was determined by measurements of the target gas pressure and temperature. For the higher gas density an error in the determination of pressure and temperature of $\pm 2.0\%$ and of $\pm 3.5\%$, respectively, was achieved, leading to a density error of $\pm 5\%$. While for the lower gas density, the pressure and temperature errors were determined to be $\pm 4.0\%$ and $\pm 5.1\%$, respectively, leading to a density error of $\pm 10\%$. For the 1.90 g/l density the result of this work is consistent with the SIDDHARTA measurement done at similar gas target density [16].

From the perspective of kaonic atoms cascade models the density region covered by these two new SIDDHARTINO measurements is of great interest since, up to now, due to the absence of data, no progress has been achieved in cascade model calculations for kaonic atoms since almost twenty years [27,14,28,29,10]. In the coming years SIDDHARTA-2 collaboration will measure the transitions yields for various kaonic atoms, by also using gas targets at various densities.

These results, including the two new kaonic helium-4 yields reported in this article, will trigger a renaissance of the cascade calculations for exotic atoms, in particular for the kaonic atoms and a better understanding of the underlying processes and physics.

CRedit authorship contribution statement

D.L. Sirghi: Formal analysis, Methodology, Software, Writing – original draft, Writing – review & editing. **H. Shi:** Formal analysis, Methodology, Resources, Software, Validation, Writing – original draft, Writing – review & editing. **C. Guaraldo:** Conceptualization, Funding acquisition, Methodology, Project administration, Supervision, Writing – original draft, Writing – review & editing. **F. Sgaramella:** Formal analysis, Methodology, Resources, Software, Validation, Writing – original draft, Writing – review & editing. **C. Amsler:** Writing – original draft, Writing – review & editing. **M. Bazzi:** Writing – review & editing. **D. Bosnar:** Writing – review & editing. **A.M. Bragadireanu:** Software, Writing – review & editing. **M. Carminati:** Writing – review & editing. **M. Cargnelli:** Methodology, Software, Writing – review & editing. **A. Clozza:** Writing – review & editing. **G. Deda:** Writing – review & editing. **L. De Paolis:** Writing – review & editing. **R. Del Grande:** Writing – review & editing. **L. Fabbietti:** Writing – review & editing. **C. Fiorini:** Funding acquisition, Methodology, Resources, Writing – review & editing. **M. Iliescu:** Conceptualization, Formal analysis, Methodology, Resources, Software,

Writing – review & editing. **M. Iwasaki:** Writing – review & editing. **J. Marton:** Writing – review & editing. **M. Miliucci:** Resources, Writing – review & editing. **P. Moskal:** Writing – review & editing. **F. Napolitano:** Writing – review & editing. **S. Niedzwiecki:** Writing – review & editing. **H. Ohnishi:** Writing – review & editing. **K. Piscicchia:** Writing – review & editing. **Y. Sada:** Writing – review & editing. **A. Scordo:** Writing – review & editing. **M. Silarski:** Writing – review & editing. **F. Sirghi:** Conceptualization, Resources, Writing – review & editing. **M. Skurzok:** Writing – review & editing. **A. Spallone:** Writing – review & editing. **K. Toho:** Writing – review & editing. **M. Tüchler:** Formal analysis, Writing – review & editing. **O. Vazquez Doce:** Formal analysis, Software, Writing – review & editing. **J. Zmeskal:** Formal analysis, Funding acquisition, Project administration, Resources, Supervision, Validation, Writing – review & editing. **C. Yoshida:** Writing – review & editing. **C. Curceanu:** Conceptualization, Formal analysis, Funding acquisition, Methodology, Project administration, Resources, Software, Supervision, Validation, Writing – original draft, Writing – review & editing.

Declaration of competing interest

The authors declare that they have no known competing financial interests or personal relationships that could have appeared to influence the work reported in this paper.

Data availability

Data will be made available on request.

Acknowledgements

We thank C. Capocchia from LNF-INFN and H. Schneider, L. Stohwasser, and D. Pristauz-Telsnigg from Stefan-Meyer-Institut for their fundamental contribution in designing and building the SIDDHARTA-2 setup. We thank as well the DAΦNE staff for the excellent working conditions and permanent support. Part of this work was supported by the Austrian Science Fund (FWF): [P24756-N20 and P33037-N]; the Croatian Science Foundation under the project IP-2018-01-8570; the EU STRONG-2020 project (Grant Agreement No. 824093), the EU Horizon 2020 project under the MSCA (Grant Agreement 754496); Japan Society for the Promotion of Science JSPS KAKENHI Grant No. JP18H05402; the Polish Ministry of Science and Higher Education grant No. 7150/E-338/M/2018 and the Polish National Agency for Academic Exchange (grant No. PPN/BIT/2021/1/00037).

References

- [1] S. Scherer, *Adv. Nucl. Phys.* 27 (2003) 277.
- [2] J. Gasser, H. Leutwyler, *Ann. Phys.* 158 (1984) 142.
- [3] V. Lyubovitskij, T. Gutsche, A. Faessler, E. Drukarev, *Phys. Rev. D* 63 (2001) 054026.
- [4] M. Merafina, et al., *Phys. Rev. D* 102 (8) (2020) 083015.
- [5] C. Curceanu, et al., *Rev. Mod. Phys.* 91 (2) (2019) 025006.
- [6] C. Curceanu, et al., *Symmetry* 12 (4) (2020) 547.
- [7] R.D. Pietri, et al., *Astrophys. J.* 881 (2) (2019) 122.
- [8] M. Leon, H.A. Bethe, *Phys. Rev.* 2 (1962) 127.
- [9] E. Borie, M. Leon, *Phys. Rev. A* 21 (1980) 1460.
- [10] T.S. Jensen, *Frascati Phys. Ser.* XXXVI (2004) 349.
- [11] T.M. Ito, et al., *Phys. Rev. C* 58 (4) (1998) 2366.

- [12] V. Popov, V. Pomerantsev, *Phys. Rev. A* 95 (2017) 022506.
- [13] A. Hirtl, D. Anagnostopoulos, D. Covita, et al., *Eur. J. Phys. A* 57 (2021) 70.
- [14] T. Koike, Y. Akaishi, *Nucl. Phys. A* 639 (1998) 521.
- [15] S. Baird, et al., *Nucl. Phys. A* 392 (1983) 297.
- [16] M. Bazzi, et al., *Eur. Phys. J. A* 50 (2014) 91.
- [17] D. Sirghi, et al., *J. Phys. G, Nucl. Part. Phys.* 49 (2022) 055106.
- [18] M. Bazzi, et al., *Phys. Lett. B* 704 (2011) 113.
- [19] M. Bazzi, et al., *Phys. Lett. B* 697 (2011) 199.
- [20] M. Bazzi, et al., *Nucl. Phys. A* 916 (2013) 30.
- [21] M. Miliucci, et al., *Condens. Matter* 4 (2019) 31.
- [22] M. Miliucci, et al., *Meas. Sci. Technol.* 33 (2022) 095502.
- [23] M. Miliucci, et al., *Meas. Sci. Technol.* 32 (2021) 095501.
- [24] M. Miliucci, et al., *Condens. Matter* 6 (2021) 47.
- [25] F. Sgaramella, et al., *Phys. Scr.* 97 (11) (2022) 114002.
- [26] M. Bazzi, et al., *Nucl. Phys. A* 954 (2016) 7.
- [27] T.P. Terada, R.S. Hayano, *Phys. Rev. C* 55 (1997) 73.
- [28] T.S. Jensen, et al., *Eur. Phys. J. D* 21 (2002) 271.
- [29] T.S. Jensen, V. Markushin, *Lect. Notes Phys.* 627 (2003) 37.